Neoplasma 2025; 72(5): 328–341

doi:10.4149/neo_2025_250619N269

WDR4 promotes glioma progression by regulating cell proliferation and cell cycle via the PI3K/Akt-CDK1/2 signaling pathway

Jun LIU[1,#], Zhe ZHANG[1,#], Shuaishuai XUE[2,#], Guanlin HUANG[3,#], Jiajie YUAN[2], Yonghua CAI[2], Zhengming ZHAN[2], Guangjie LIU[2], Bei ZHANG[4], Xinyun YE[3,*], Ye SONG[3,5,*], Peng LI[2,*], Hua GUO[1,*]

[1]Department of Neurosurgery, The 2nd Affiliated Hospital, Jiangxi Medical College, Nanchang University, Nanchang, Jiangxi, China; [2]Department of Neurosurgery, Nanfang Hospital of Southern Medical University, Guangzhou, Guangdong, China; [3]Department of Neurosurgery, Ganzhou People's Hospital, Ganzhou, Jiangxi, China; [4]Department of Biostatistics, Virginia Commonwealth University, Richmond, Virginia, United States; [5]Department of Neurosurgery, Guangzhou Women and Children's Medical Center, Guangzhou, Guangdong, China

**Correspondence: yexinyun1270@163.com; songye@smu.edu.cn; zhimeng_li@163.com; ndefy02014@ncu.edu.cn*
[#]Contributed equally to this work.

Received June 19, 2025 / Accepted September 26, 2025

WD Repeat Domain 4 (WDR4) is integral to the development and progression of various cancers; however, its specific role and underlying molecular mechanisms in glioma remain inadequately elucidated. This study undertook an analysis of WDR4 expression levels in glioma and normal brain tissues utilizing publicly accessible datasets from TCGA and GTEx project, with further validation conducted through the GEPIA and the HPA databases. Prognostic significance was assessed using Kaplan-Meier survival analysis and multivariate Cox regression models. Cellular functions were investigated through CCK-8 viability assays, colony formation assays, and cell cycle analysis, while the tumorigenic potential *in vivo* was corroborated using a nude mouse xenograft model. The findings revealed a significant upregulation of WDR4 in both glioma tissues and cell lines. Elevated WDR4 expression correlated with reduced overall survival and emerged as an independent prognostic factor. Functional assays indicated that WDR4 silencing markedly inhibited glioma cell proliferation, induced G1 phase cell cycle arrest, and resulted in the downregulation of CDK1 and CDK2 protein expression. Further co-expression analysis, GSEA, KEGG pathway enrichment, and western blotting suggested that WDR4 may exert its oncogenic effects through activation of the PI3K/Akt signaling pathway. In conclusion, WDR4 is highly expressed in glioma and promotes tumor progression via the PI3K/Akt-CDK1/2 signaling axis. These findings indicate that WDR4 may serve as a potential prognostic biomarker and therapeutic target in glioma.

Key words: WDR4; glioma; cell proliferation; cell cycle regulation; PI3K/Akt signaling pathway; CDK1/2

Glioma represents a common form of cancer within the central nervous system, classified by the World Health Organization into grades 1 through 4 [1, 2]. Standard treatment modalities encompass surgical resection, chemotherapy, and radiotherapy. Despite these interventions, clinical outcomes and long-term survival rates remain suboptimal [3, 4]. Although numerous studies have identified tumor suppressor genes and oncogenes implicated in glioma pathogenesis, these findings are insufficient for precise diagnosis and effective treatment. Consequently, further research is imperative to elucidate underlying biological mechanisms, identify novel therapeutic targets, and discover effective biomarkers for gliomas.

WD repeat domain 4 (WDR4), a member of the WD-repeat protein family, plays a crucial role in various cellular processes, including cell cycle progression, signal transduction, genetic regulation, and programmed cell death [5, 6]. Proteins containing WD-repeats are characterized by a circularized beta-propeller structure, which serves as a foundation for interactions with scaffold proteins and potential targets for small molecules [6–8]. WDR4 has been identified as a significant contributor to the development and progression of multiple cancer types [9–12]. In the context of hepatocellular carcinoma, WDR4 facilitates the translation of CCNB1, thereby promoting increased proliferation, metastasis, and resistance to sorafenib [13]. Additionally, the WDR4 oncoprotein impedes promyelocytic leukemia through ubiquitination, thereby advancing lung cancer by creating a pro-metastatic and immunesuppressive environment [14]. In bladder cancer, WDR4

downregulates ARRB2, thus promoting cancer progression and lymphatic metastasis [15]. Previous studies have suggested that WDR4 may function as a susceptibility gene in glioma [16, 17]. However, the precise role of WDR4 in regulating the biological behavior of glioma cells and the underlying molecular mechanisms remain largely unclear, warranting further investigation.

This study investigates the role of WDR4 in glioma using both bioinformatics analyses and experimental validation. Bioinformatics findings revealed that the mRNA and protein levels of WDR4 are significantly elevated in glioma tissue samples and cell lines. These elevated levels are highly correlated with clinical characteristics and poor prognoses in glioma patients. Notably, experimental results demonstrated that WDR4 knockdown significantly inhibited glioma cell growth in both *in vitro* and *in vivo* models. Furthermore, our findings indicate that WDR4 facilitates glioma cell proliferation via the PI3K/Akt-CDK1/2 signaling pathway *in vitro*. Consequently, WDR4 may serve as a potential target for guiding therapeutic strategies in glioma treatment.

Materials and methods

Clinical samples data collection. Gene expression profiling was conducted for glioma samples (n=689) obtained from The Cancer Genome Atlas (TCGA) and normal brain tissues (n=1,157) from the Genotype-Tissue Expression (GTEx) database using the GEPIA online tool (https://gepia2.cancer-pku.cn/#analysis; accessed on October 10, 2023). Validation of WDR4 protein expression was performed using the Human Protein Atlas (HPA) database (https://www.proteinatlas.org; accessed on October 20, 2023). The expression levels of WDR4 were analyzed in both glioma and non-cancerous brain tissues. In addition, the association between WDR4 expression and glioma patient prognosis was investigated.

Cell lines and cell culture. Normal human astrocyte (NHA) and the human glioma cell lines HS683, SW1783, LN229, U87, and U251 were obtained from the American Type Culture Collection (ATCC, Manassas, VA, USA). The human embryonic kidney epithelial cell line HEK293T, commonly used for lentiviral packaging, was obtained from the Shanghai Institute of Cell Biology, Chinese Academy of Sciences (Shanghai, China). All cell lines were cultured in Dulbecco's Modified Eagle Medium (DMEM; high glucose, Gibco, USA) supplemented with 10% fetal bovine serum (FBS; Gibco, USA) at 37 °C in a humidified incubator containing 5% CO_2. Cells were routinely passaged at ~80–90% confluence using 0.25% trypsin-EDTA (Gibco) and were used in logarithmic growth phase for all subsequent experiments.

Model-independent prognostic analysis of WDR4. Survival analysis, as well as univariate and multivariate Cox proportional hazards regression models, were performed to evaluate the clinical relevance of WDR4 expression in glioma patients using comprehensive clinical data obtained from The Cancer Genome Atlas (TCGA) database. Specifically, associations between WDR4 expression and key clinical parameters, including patient age, gender, World Health Organization (WHO) grade, isocitrate dehydrogenase (IDH) mutation status, and 1p/19q codeletion status, were assessed. All statistical analyses were conducted using the "survival" package in R (version 4.0.2).

Lentivirus packaging and infection targeting WDR4. To generate lentiviral particles carrying shRNA targeting human WDR4, two specific shRNA sequences (shWDR4-1: 5'-AGCATAACTGTAACCCTAATA-3';shWDR4-2:5'-CCGCATAGCATCGAGTCTTTC-3') were cloned into the pLKO.1-puro vector. HEK293T cells were co-transfected with pLKO.1-shWDR4, psPAX2, and pMD2.G plasmids using polyethyleneimine (PEI, Sigma-Aldrich). After 48 h, viral supernatants were collected, filtered through a 0.45 μm filter, and used to transduce LN229 and U251 cells in the presence of 8 μg/ml polybrene. For overexpression of WDR4, the full-length human WDR4 cDNA (corresponding to the complete coding sequence, NM_018669.6) was subcloned into the pLVX-Puro lentiviral expression vector (Clontech). Lentiviral particles were generated by co-transfecting HEK293T cells with pLVX-WDR4, psPAX2, and pMD2.G using PEI. Viral supernatants were harvested at 48- and 72-h post-transfection and used to transduce SW1783 cells. Following transduction, cells were selected with puromycin (2 μg/ml) for 3–5 days to establish stable cell lines. All shRNA and overexpression plasmids were obtained from GeneChem (Guangzhou, China).

Western blot. Cells were washed twice with ice-cold phosphate-buffered saline (PBS) and lysed on ice using radioimmunoprecipitation assay (RIPA) buffer supplemented with protease and phosphatase inhibitors (Beyotime, Shanghai, China). Protein concentrations were determined using the BCA Protein Assay Kit (Thermo Fisher Scientific, USA). Equal amounts of protein were separated by sodium dodecyl sulfate-polyacrylamide gel electrophoresis (SDS-PAGE) and transferred onto polyvinylidene fluoride (PVDF) membranes. Membranes were blocked with 5% skim milk in PBST (PBS containing 0.1% Tween-20) for 2 h at room temperature and then incubated overnight at 4 °C with primary antibodies. After three washes with PBST, membranes were incubated with horseradish peroxidase (HRP)-conjugated secondary antibodies for 1 h at room temperature, followed by three additional washes with PBST. Protein bands were visualized using enhanced chemiluminescence (ECL) detection reagent (Millipore, USA) and captured with an automated chemiluminescence imaging system. All experiments were performed in triplicate. Primary antibodies used included anti-p-Akt (#4060, 1:1000), Akt (#9272, 1:1000), and CDK2 (#18048, 1:1000) (all from Cell Signaling Technology, USA), as well as WDR4 (#ARC2292, 1:1000) and CDK1 (#MA5-11472, 1:1000) (Thermo Fisher Scientific, USA). HRP-conjugated secondary antibodies (#31460 and #31430, 1:10000) were also obtained from Thermo Fisher Scientific.

Cell viability assay. In the Cell Counting Kit-8 (CCK8, Dojindo, Japan) assay, LN229, U251, and SW1783 cells stably transduced with the indicated lentiviral constructs were seeded into 96-well plates at a density of 1,000 cells per well in 100 µl of complete growth medium (DMEM supplemented with 10% FBS and 1% penicillin-streptomycin). Cells were cultured at 37 °C in a humidified atmosphere with 5% CO_2. At days 1, 3, 5, and 7 after seeding, 10 µl of CCK-8 reagent was added to each well, followed by incubation for 2 h at 37 °C. The absorbance at 450 nm was measured using a microplate reader (Thermo Fisher, USA). The optical density (OD) values were used to evaluate cell viability and proliferation.

Cell proliferation assay. N229, U251, and SW1783 cells stably transduced with either control or WDR4-targeting shRNA (or overexpressing WDR4) were seeded into 6-well plates at a density of 500 cells/well in triplicate. Cells were cultured in complete medium (DMEM supplemented with 10% FBS and 1% penicillin-streptomycin) with or without puromycin (2 µg/ml, depending on stable selection) at 37 °C in a humidified incubator with 5% CO_2 for 10–14 days, allowing visible colonies to form. After being washed, fixed, and stained with crystal violet (#548-62-9, Sigma-Aldrich), the clones were then photographed using a high-resolution digital camera. The number of colonies formed was analyzed by ImageJ software (version 1.51j8).

Cell cycle assay. Cell cycle distribution was analyzed by flow cytometry using the Cell Cycle and Apoptosis Analysis Kit (Beyotime, China) according to the manufacturer's instructions. Briefly, transfected U251, LN229, and SW1783 cells were harvested by centrifugation at 300×g for 5 min, washed once with cold PBS, and fixed in ice-cold 70% ethanol at 4 °C overnight. After fixation, cells were washed with PBS and incubated in a staining solution containing RNase A (100 µg/ml) and 0.5% Triton X-100 for 30 min at 37 °C in the dark. Subsequently, cells were stained with propidium iodide (PI, 50 µg/ml) for 30 min at room temperature in the dark. DNA content was analyzed by flow cytometry, and data were processed using FlowJo software (version X.0.7, TreeStar, Ashland, OR, USA).

5-bromo-2'-deoxyuridine (BrdU) assay. Proliferation was measured using a BrdU assay kit (Applygen, China), according to the manufacturer's instructions with slight modifications. Briefly, transfected U251, LN229, and SW1783 cells were seeded into 6-well plates and allowed to adhere overnight. Cells were incubated with BrdU at a final concentration of 10 µM for 2 h at 37 °C. After labeling, cells were fixed with 4% paraformaldehyde for 15 minutes at room temperature, permeabilized with 0.1% Triton X-100 for 10 min, and then treated with 1.5 M HCl for 20 min at room temperature to denature DNA. Following DNA denaturation, cells were washed and blocked in 1% BSA for 30 min, then incubated with anti-BrdU monoclonal antibody (1:100 dilution, #1170376, Roche) at 4 °C overnight. After washing, appropriate fluorophore-conjugated secondary antibodies were applied for 1 h at room temperature. Nuclei were counterstained with DAPI. Images were captured using a fluorescence microscope, and BrdU-positive cells were quantified from three randomly selected fields per sample.

Gene enrichment analysis. To investigate the biological functions of WDR4 at varying expression levels, we conducted Gene Ontology (GO) and Kyoto Encyclopedia of Genes and Genomes (KEGG) pathway enrichment analyses using the Database for Annotation, Visualization, and Integrated Discovery (DAVID) (https://david.ncifcrf.gov/). GO analysis results were categorized into three domains: Biological Processes (BP), Molecular Functions (MF), and Cellular Components (CC). The top eight significantly enriched terms in each category were visualized using bar plots. Additionally, the top eight tumor-related signaling pathways identified by KEGG enrichment analysis were also illustrated. To further explore functional differences between glioma and normal brain tissues, Gene Set Enrichment Analysis (GSEA) was performed (https://www.gsea-msigdb.org/gsea/index.jsp). The Normalized Enrichment Score (NES) and False Discovery Rate (FDR) were calculated to assess the significance and reliability of the enrichment results.

Construction of tumor models in nude mice. To establish an orthotopic glioblastoma model, U251 cells (5×10^5 cells in 5 µl PBS) stably transduced with either shWDR4 or shNC control lentivirus were implanted into the brains of nude mice (male, 4–6 weeks old, n = 7/group) via stereotactic intracranial injection. On day 15 post-injection, intracranial tumor growth was monitored using a bioluminescent *in vivo* imaging system (IVIS Spectrum, PerkinElmer, USA) after intraperitoneal injection of D-luciferin (150 mg/kg). Mice were anesthetized and imaged under standardized settings. For histological examination, mouse brains were harvested, fixed in 4% paraformaldehyde, embedded in paraffin, and sectioned for hematoxylin and eosin (H&E) staining. For survival analysis, a separate cohort of mice (n = 7/group) was intracranially implanted with U251 cells as described above and monitored daily. Mice were euthanized when they exhibited neurological symptoms or reached a moribund state. Kaplan-Meier survival curves were generated and analyzed accordingly.

Ethics approval and consent to participate. The animal studies were performed according to the guidelines and approval of the Ethical Committee of Nanfang Hospital, Southern Medical University. (Approval No. IACUC-LAC-20230703-004).

Statistical analysis. All p-values were two-sided, and values less than 0.05 were considered statistically significant. Logistic regression analysis was employed to assess the associations between WDR4 expression levels and various clinical parameters. Overall survival (OS) was analyzed using multivariate Cox proportional hazards regression to evaluate the prognostic impact of WDR4 expression and other clinicopathological factors. Quantitative data were expressed as mean ± standard deviation (SD). Statistical comparisons

between groups were performed using independent t-tests or one-way analysis of variance (ANOVA), as appropriate.

Results

Elevated WDR4 expression in glioma correlates with poor patients' prognosis. We analyzed 689 glioma samples of varying grades from TCGA database and 1,157 normal brain tissue samples from the GTEx database. The mRNA expression of WDR4 was significantly upregulated in both glioblastoma multiforme (GBM) and low-grade gliomas (LGG) compared to normal brain tissues (Figure 1A). Kaplan-Meier survival analysis demonstrated that elevated WDR4 expression was significantly associated with poorer OS in glioma patients ($p<0.001$, Figure 1B). Furthermore, GBM samples exhibited higher WDR4 expression levels relative to LGG samples and adjacent normal brain tissues, a finding that was corroborated by protein expression data from the HPA database (Figures 1C, 1D). Consistently, WDR4 protein levels were markedly higher in high-grade glioma cell lines (U251, U87, and LN229) compared to LGG cell lines (HS683 and SW1783) and NHA, as shown by western blot analysis (Figures 1E, 1F). Immunofluorescence confocal microscopy revealed predominant nuclear localization of WDR4 in U251 and LN229 cells (Figure 1G). Collectively, these results suggest that WDR4 is overexpressed in glioma and may contribute to its malignant progression.

The expression of WDR4 is linked to the clinical features of patients with glioma. We investigated the association between WDR4 expression and various clinical features in glioma patients, including tumor grade, OS events, IDH mutation status, patient age, 1p/19q codeletion status, and gender. High-grade gliomas exhibited significantly elevated WDR4 expression compared to LGG (Figure 2A). Additionally, WDR4 expression was markedly higher in patients who had experienced OS events (deceased) than in those who remained alive (Figure 2B). WDR4 expression was also significantly increased in IDH wild-type patients compared to those harboring IDH mutations (Figure 2C). Furthermore, glioma patients over the age of 60 exhibited higher WDR4 expression than younger patients (Figure 2D). However, no statistically significant differences in WDR4 expression were observed between male and female patients, nor between patients with and without 1p/19q codeletion (Figures 2E, 2F). To determine whether WDR4 serves as an independent prognostic factor in glioma, we performed both univariate and multivariate Cox regression analyses. WDR4 expression remained significantly associated with OS after adjusting for other clinical covariates. Specifically, both univariate and multivariate analyses identified age ($p_1<0.001$, $p_2=0.008$), tumor grade ($p_1<0.001$, $p_2<0.001$), IDH mutation status ($p_1<0.001$, $p_2<0.001$), and 1p/19q codeletion status ($p_1<0.001$, $p_2=0.024$) as significant prognostic indicators (Table 1). Furthermore, receiver operating characteristic (ROC) curve analysis revealed that WDR4 expression possesses strong diagnostic potential, with an area under the curve (AUC) of 0.867 (Figure 2G). Collectively, these findings suggest that elevated WDR4 expression is associated with adverse clinical outcomes and may serve as an independent prognostic biomarker for glioma.

WDR4-related functional enrichment analyses. GSEA was performed to explore the WDR4-associated signaling

Table 1. Univariate and multivariate analyses of clinicopathological parameters (including WDR4 expression) in patients with glioma.

Characteristics	Total (N)	Hazard ratio (95% CI)	P_1-value	Hazard ratio (95% CI)	P_2-value
Age	695				
≤60	552	Reference			
>60	143	4.668 (3.598–6.056)	**<0.001**	1.526 (1.115-2.089)	**0.008**
Gender	695				
female	297	Reference			
male	398	1.262 (0.988–1.610)	0.062	1.312 (0.998-1.724)	0.052
WHO grade	634				
G2 and G3	466	Reference			
G4	168	9.496 (7.212–12.503)	**<0.001**	2.386 (1.651-3.448)	**<0.001**
IDH status	685				
wt	246	Reference			
mut	439	0.117 (0.090–0.152)	**<0.001**	0.284 (0.191-0.422)	**<0.001**
1p/19q codeletion	688				
codel	170	Reference			
non-codel	518	4.428 (2.885–6.799)	**<0.001**	1.733 (1.045-2.872)	**0.033**
WDR4	695				
low	348	Reference			
high	347	2.343 (1.827–3.004)	<0.001	1.408 (1.045-1.896)	**0.024**

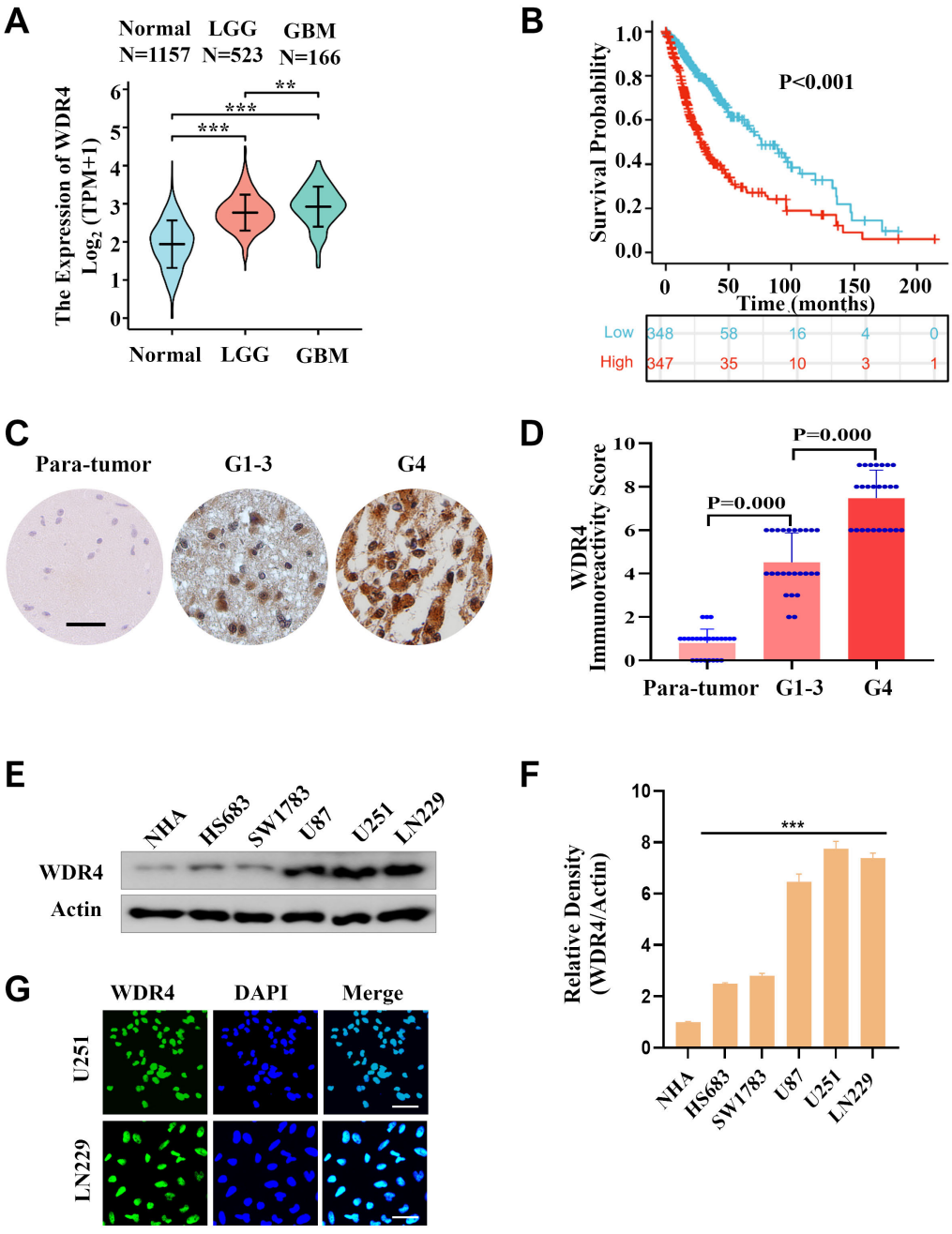

Figure 1. WDR4 mRNA and protein expression between normal and glioma samples and cell lines, and OS in glioma patients. A) The mRNA expression of WDR4 in normal and glioma tissues from TCGA database. B) Kaplan-Meier analyses of the OS of patients in gliomas with high and low WDR4 expression. p<0.001. C, D) Immunohistochemical staining and quantification of WDR4 in para-tumor and glioma tissues. E, F) The protein expression and quantification of WDR4 in human astrocyte cell lines, HS683, SW1783, U87, U251, and LN229 by western blotting. G) Immunofluorescent staining of WDR4 in U251 and LN229. Bar = 200 μm.

pathways in glioma by stratifying samples into high and low WDR4 expression groups. The analysis revealed significant enrichment differences in both GO and KEGG datasets (FDR < 0.05, p < 0.05). Specifically, gene sets such as REACTOME_CELL_CYCLE_MITOTIC, KEGG_CELL_CYCLE, and WP_CELL_CYCLE were significantly enriched in the high WDR4 expression group, as indicated by NES, FDR, and p-values (Figures 3A–3C). To further investigate the biological functions regulated by WDR4, GO and KEGG enrichment analyses were conducted using differentially expressed genes

(DEGs) between high and low WDR4 expression groups derived from TCGA dataset. The GO terms were categorized into three domains: BP, CC, and MF.

In the BP category, DEGs were primarily enriched in pathways related to nuclear division, chromosome segregation, mitotic nuclear division, extracellular matrix organization, and regulation of cell cycle progression (Figure 3D). In terms of CC, genes were significantly associated with components such as the spindle, centromeric chromosome, microtubules, protein–DNA complex, and DNA packaging complex (Figure 3E). Regarding MF, enrichment was observed in functions such as DNA-binding transcription activator activity (RNA polymerase II-specific), metal ion transmembrane transporter activity, extracellular matrix structural constituent, and microtubule binding (Figure 3F). KEGG pathway enrichment analysis showed that DEGs were significantly involved in pathways including the PI3K/Akt signaling pathway, cell cycle regulation, transcriptional

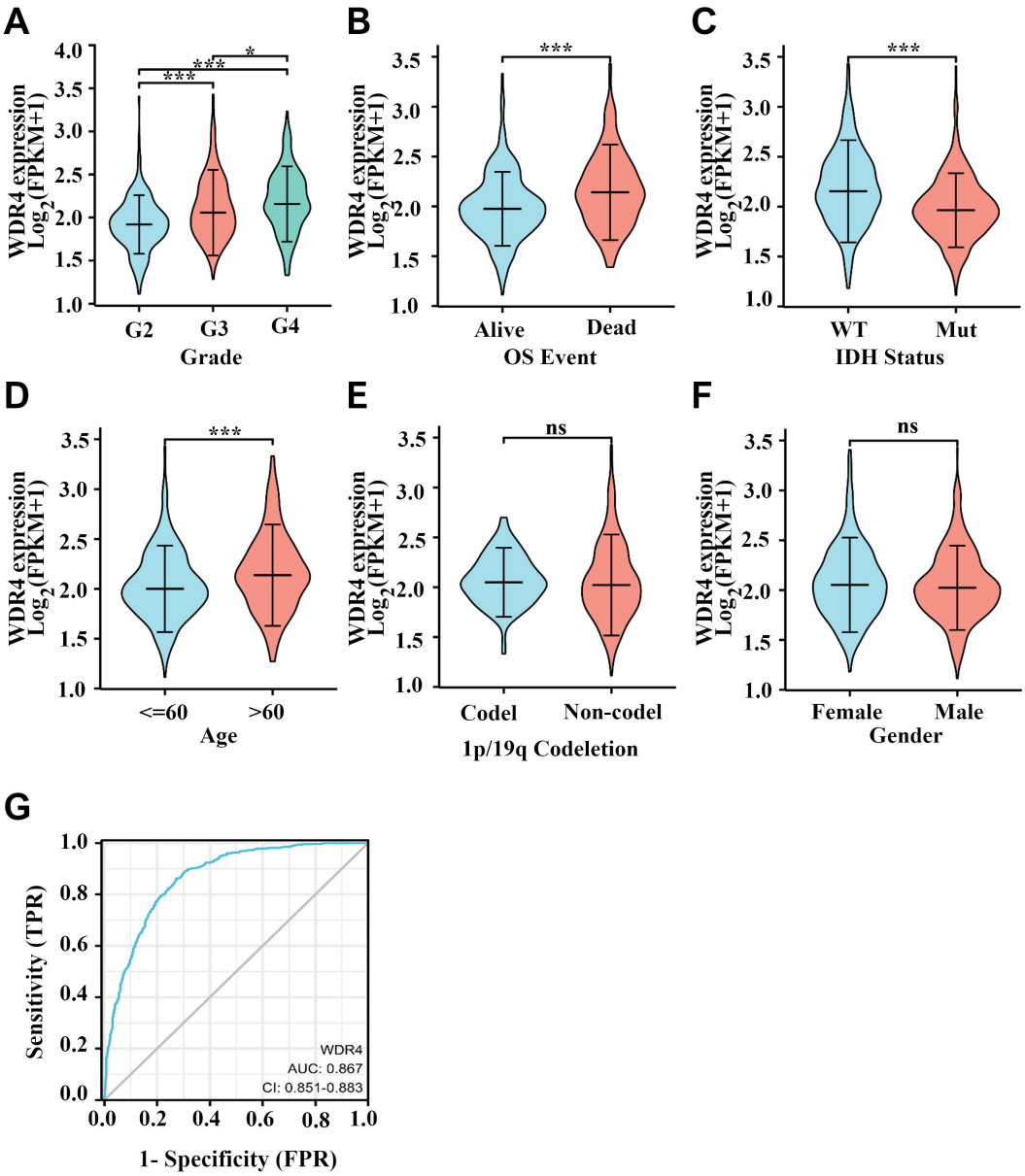

Figure 2. The associations between WDR4 mRNA and clinic characteristics. A) WDR4 mRNA expression level in different grades of glioma patients. B) WDR4 mRNA expression was high in patients with short survival. C) WDR4 mRNA expression was high in IDH wild-type status. D) WDR4 mRNA expression was high in patients over 60 years old. E) WDR4 mRNA expression had no significance in 1p/19q codeletion status glioma tissues compared to non-codel status. F) WDR4 mRNA expression was similar in different genders of glioma. G) The ROC curve shows the good diagnostic value of WDR4 in glioma.

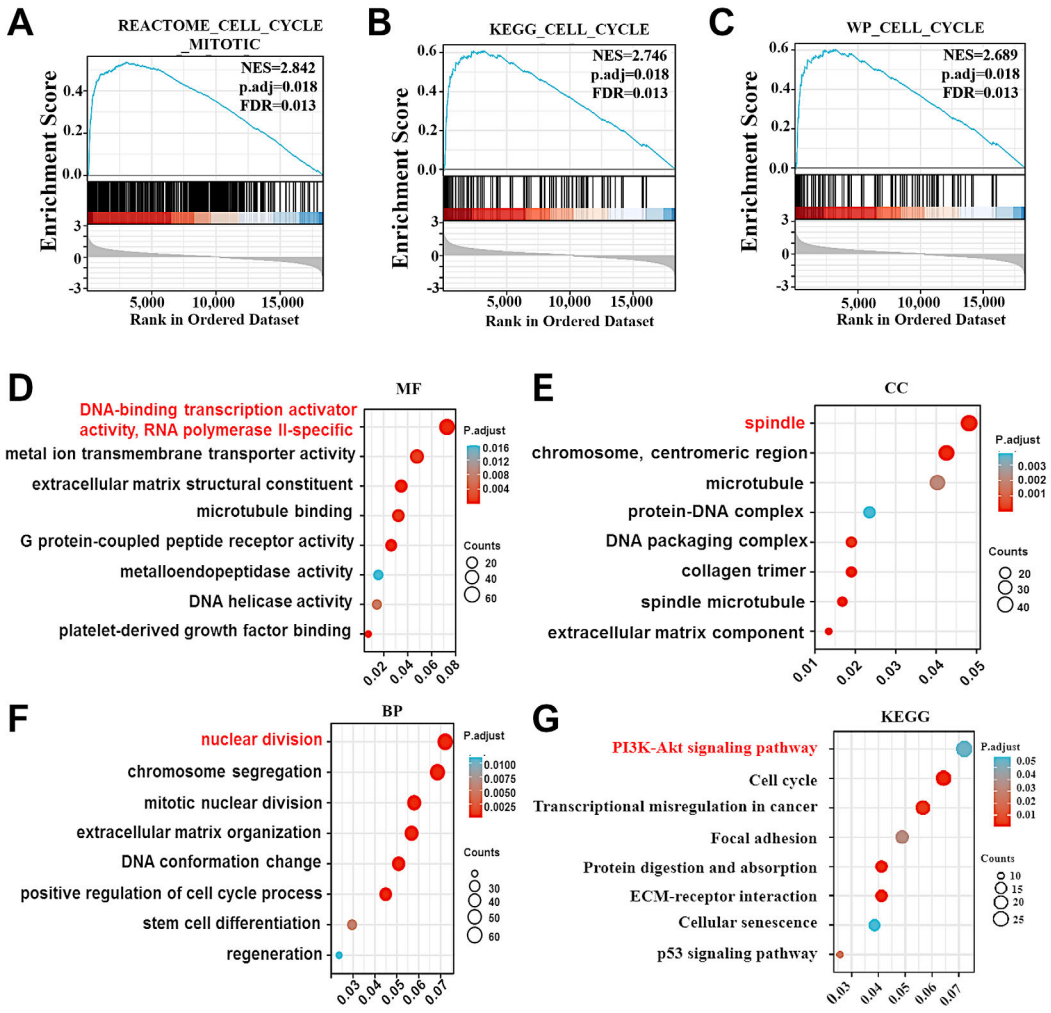

Figure 3. Enrichment analysis of WDR4 in glioma from TCGA database by GSEA, GO, and KEGG. A–C) The cell cycle was enriched by GSEA. D–F) GO functional enrichment related to WDR4 with its co-expressed mRNA. G) KEGG pathway related to WDR4 with its co-expressed mRNA.

misregulation in cancer, focal adhesion, and protein digestion and absorption (Figure 3G). These results collectively suggest that WDR4 may play a crucial role in glioma progression by modulating key signaling pathways and biological processes associated with cell cycle regulation and tumor microenvironment remodeling.

WDR4 induces glioma cell viability and proliferation *in vitro*. To investigate the functional role of WDR4 in glioma, we employed two independent shRNAs targeting WDR4 mRNA to silence its expression in U251 (Figure 4A) and LN229 (Figure 4B) cells. Knockdown of WDR4 significantly reduced cell viability in both U251 (Figure 4D) and LN229 (Figure 4E) cell lines, whereas overexpression of WDR4 in SW1783 cells (Figure 4C) exerted the opposite effect, promoting cell survival (Figure 4F). Colony formation assays further confirmed these findings, showing that WDR4 depletion markedly suppressed colony-forming ability in U251 (Figures 4G, 4J) and LN229 (Figures 4H, 4K) cells. In contrast, WDR4 overexpression significantly enhanced colony formation in SW1783 cells (Figures 4I, 4L). Collectively, these results demonstrate that WDR4 promotes glioma cell viability and proliferation *in vitro*.

WDR4 promotes the tumorigenicity of glioma cells *in vivo*. To further evaluate whether WDR4 promotes glioma cell proliferation *in vivo*, an intracranial xenograft mouse model was established. Silencing of WDR4 resulted in a significant reduction in tumor size compared to the control group (Figures 5A–5C). Moreover, survival analysis revealed that WDR4 knockdown markedly prolonged the OS of tumor-bearing mice (Figure 5D). The results of these experiments demonstrate the role of WDR4 in promoting glioma malignant progression *in vivo*.

WDR4 upregulates CDK1 and CDK2 through the PI3K/Akt signaling pathway. To further elucidate the

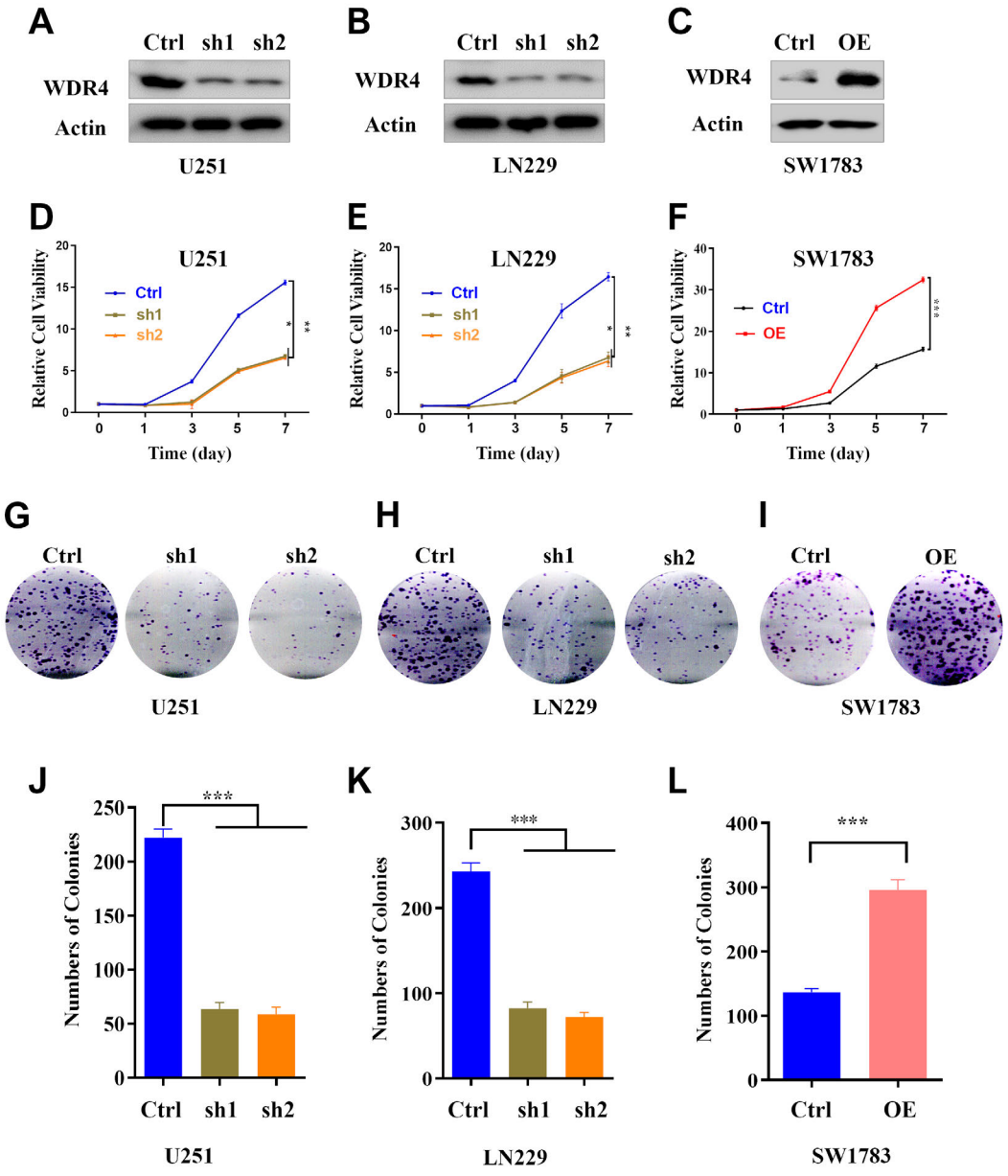

Figure 4. WDR4 induces glioma cell viability and proliferation *in vitro*. A, B) WDR4 was knocked down by shRNAs in U251 and LN229 cells as detected by western blotting. C) WDR4 was overexpressed in SW1783 cells as detected by western blotting. D–F) The CCK-8 assay was used to explore the viability of cells after knockdown or overexpression of WDR4 in cell lines. G–I) Colony formation assay was used for the evaluation of the proliferation of cells with knockdown or overexpression of WDR4. J–L) The ratio of colony formation was quantified and calculated as histograms.

genes positively associated with WDR4 expression, a Pearson correlation analysis was conducted, considering the established link between WDR4 expression and cell cycle regulation in glioma. The analysis indicated a positive correlation between WDR4 expression and the expression levels of CDK1, CDK2, AKT1, and AKT2 (Figures 6A–6D). Subsequent KEGG pathway analysis revealed a significant association between WDR4 and the PI3K/AKT signaling pathway, which is extensively implicated in cell cycle regulation across various cancers, including glioma. Based on these findings, we hypothesized that WDR4 may modulate glioma cell cycle progression through the PI3K/AKT pathway, thereby affecting tumor cell proliferation. To evaluate this hypothesis, we examined the activation status of the PI3K/AKT pathway following the silencing of WDR4. The knockdown of WDR4 in U251 and LN229 cells resulted in diminished activation of the PI3K/AKT pathway, as demonstrated by reduced levels of phosphorylated AKT (p-AKT) and the downregulation of CDK1 and CDK2 (Figures 6E, 6F).

WDR4 knockdown induces cell-cycle arrest at G1/S phase and inhibits BrdU incorporation. To examine the impact of WDR4 modulation on cell cycle dynamics, we conducted flow cytometric analyses on glioma cells subjected to either WDR4 knockdown or overexpression. In U251 and LN229 cell lines, WDR4 knockdown resulted in a pronounced G1/S phase arrest, whereas WDR4 overexpression in SW1783 cells facilitated G2/M phase progression (Figures 7A–7E). To further evaluate proliferative activity, we employed BrdU incorporation assays in conjunction with immunofluorescence staining and flow cytometry. The findings revealed an increase in BrdU incorporation in SW1783 cells overexpressing WDR4, indicative of enhanced DNA synthesis and proliferation. In contrast, BrdU incorporation was significantly diminished in U251 and LN229 cells with WDR4 knockdown (Figures 8A–8F). Collectively, these results suggest that WDR4 is pivotal in regulating cell cycle progression in glioma cells, with its downregulation contributing to G1/S arrest, while overexpression facilitates G2/M transition and promotes cellular proliferation.

Discussion

WDR4 is a critical component of the RNA N7-methylguanosine (m7G) methyltransferase complex, and increasing evidence has demonstrated its oncogenic potential in various malignancies [18–22]. Elevated WDR4 expression has been observed across multiple cancer types, including bladder cancer, esophageal squamous cell carcinoma, hepatocellular carcinoma, and lung cancer, where it contributes to enhanced tumor cell proliferation and migration [13–15, 23]. A pan-cancer analysis of 33 human cancer types has shown a significant association between high WDR4 expression and poor clinical outcomes [17, 24]. Interestingly, the function of WDR4 appears to be context-dependent, with heterogeneous roles across different tumor types. While it is predominantly described as an oncogene, certain studies suggest dual functions, including tumor-suppressive effects under specific conditions. As our understanding of WDR4's role in cancer biology deepens, its potential as both a prognostic and predictive biomarker is gaining increasing attention.

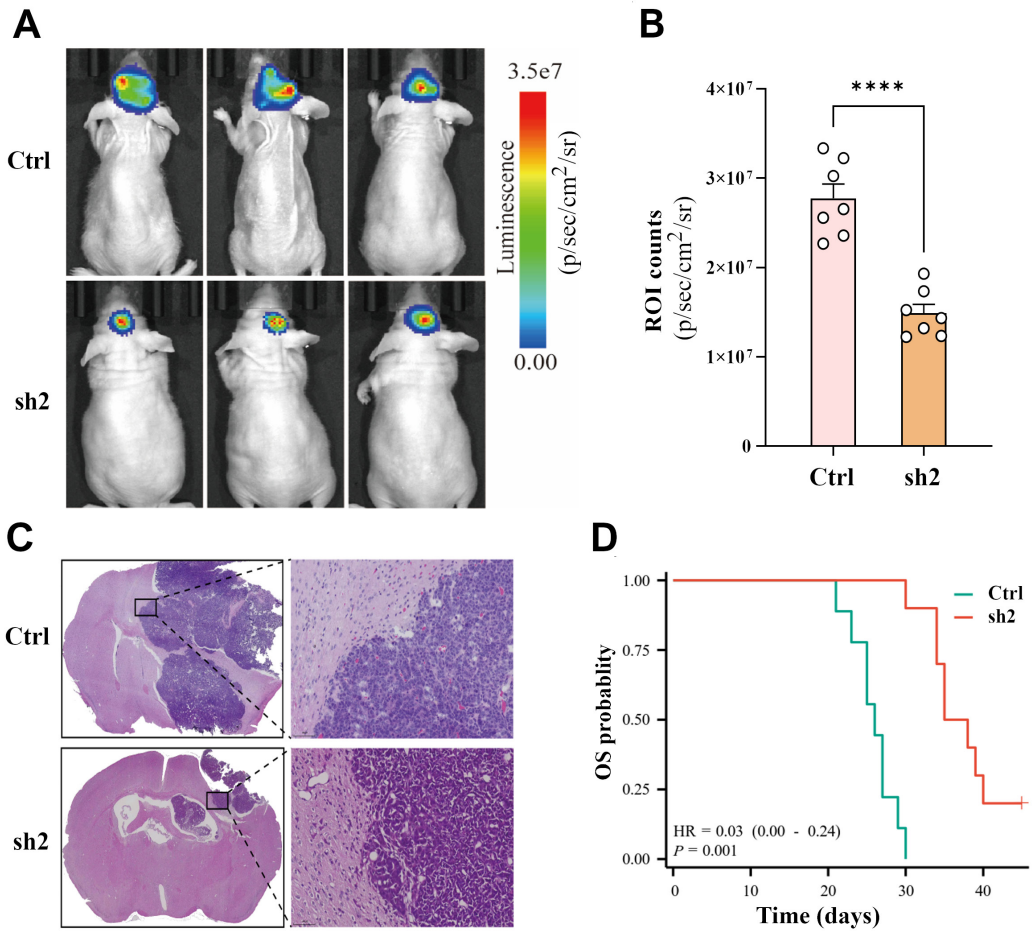

Figure 5. Detection of tumorigenesis in nude mouse *in situ* implantation tumor model with stable knockdown of WDR4. A) Representative images of bioluminescence in mice at day 15 post-implantation. B) Quantitative bioluminescence analysis of all mice at day 15 post-implantation. C) Images of the H&E staining in the local area enlargement of the tumor. Bar = 50 μm. D) Different groups' OS rates.

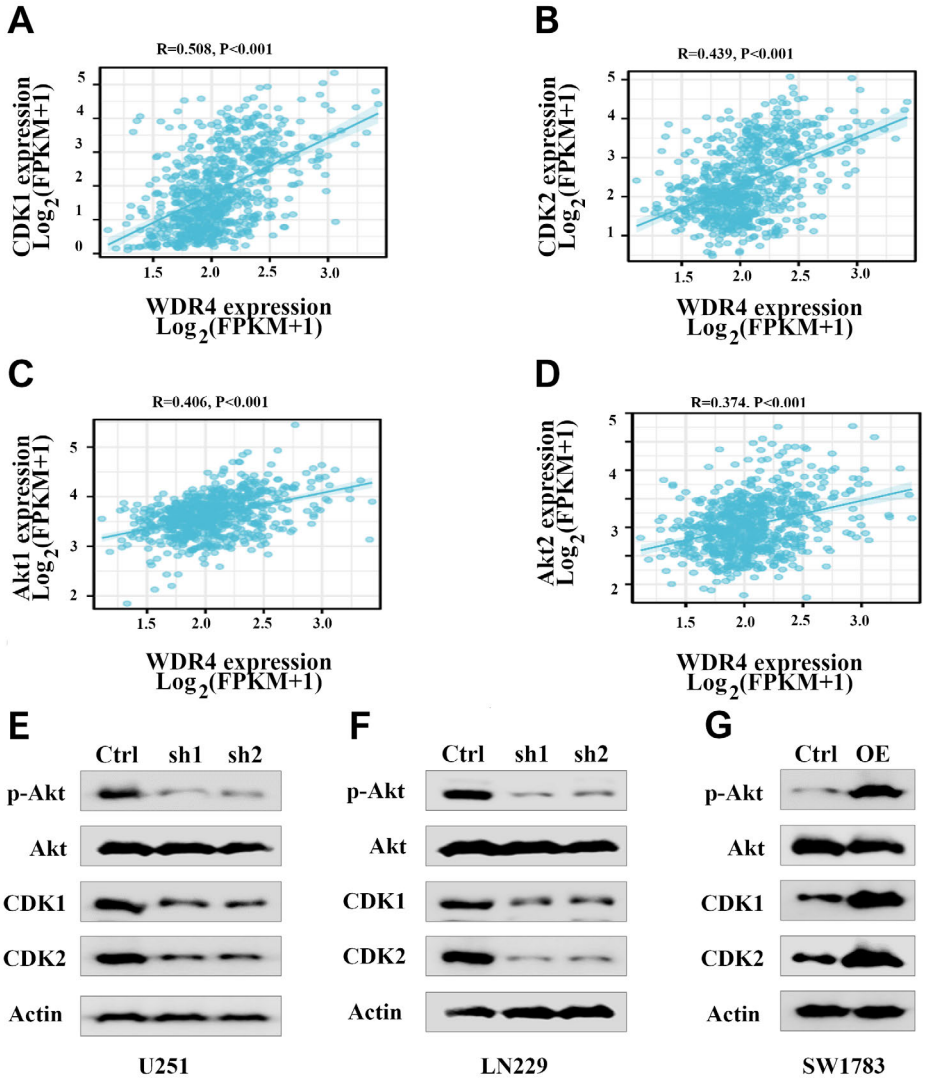

Figure 6. WDR4 upregulates CDK1 and CDK2 through the PI3K/Akt signaling pathway. A–D) Correlation analysis between WDR4 and CDK1, CDK2, Akt1, and Akt2 mRNA expression levels according to TCGA database. E, F) CDK1, CDK2, Akt, and P-Akt were detected by western blotting after knockdown of WDR4 in U251 and LN229 cells. G) CDK1, CDK2, Akt, and P-Akt were detected by western blotting after WDR4 overexpression in SW1783 cells.

In glioma, WDR4 has been implicated as a susceptibility gene contributing to tumorigenesis [16, 24], but its precise function and the underlying molecular mechanisms remain largely unexplored.

In the present study, transcriptomic data from TCGA and GTEx revealed that WDR4 is significantly upregulated in glioma tissues compared to adjacent non-tumorous or normal brain tissues. Moreover, a stepwise increase in WDR4 expression was observed with advancing tumor grade. Consistent with this, WDR4 expression was elevated in glioma cell lines relative to NHA, reinforcing the notion that WDR4 may play a functional role in glioma development. Survival analysis indicated that high WDR4 expression was significantly associated with poorer prognosis in glioma patients, suggesting its utility as a prognostic biomarker. Moreover, WDR4 expression was significantly correlated with several clinical parameters influencing glioma prognosis, including patient age, tumor grade, and IDH mutation status. However, no statistically significant associations were observed between WDR4 expression and either patient gender or 1p/19q codeletion status. To further elucidate the clinical significance of WDR4, both univariate and multivariate Cox regression analyses were performed, which confirmed that high WDR4 expression serves as an independent risk factor for unfavorable outcomes in glioma patients. These findings imply that WDR4 not only participates in glioma tumorigenesis and progression but may also function as an oncogene driving malignant behavior.

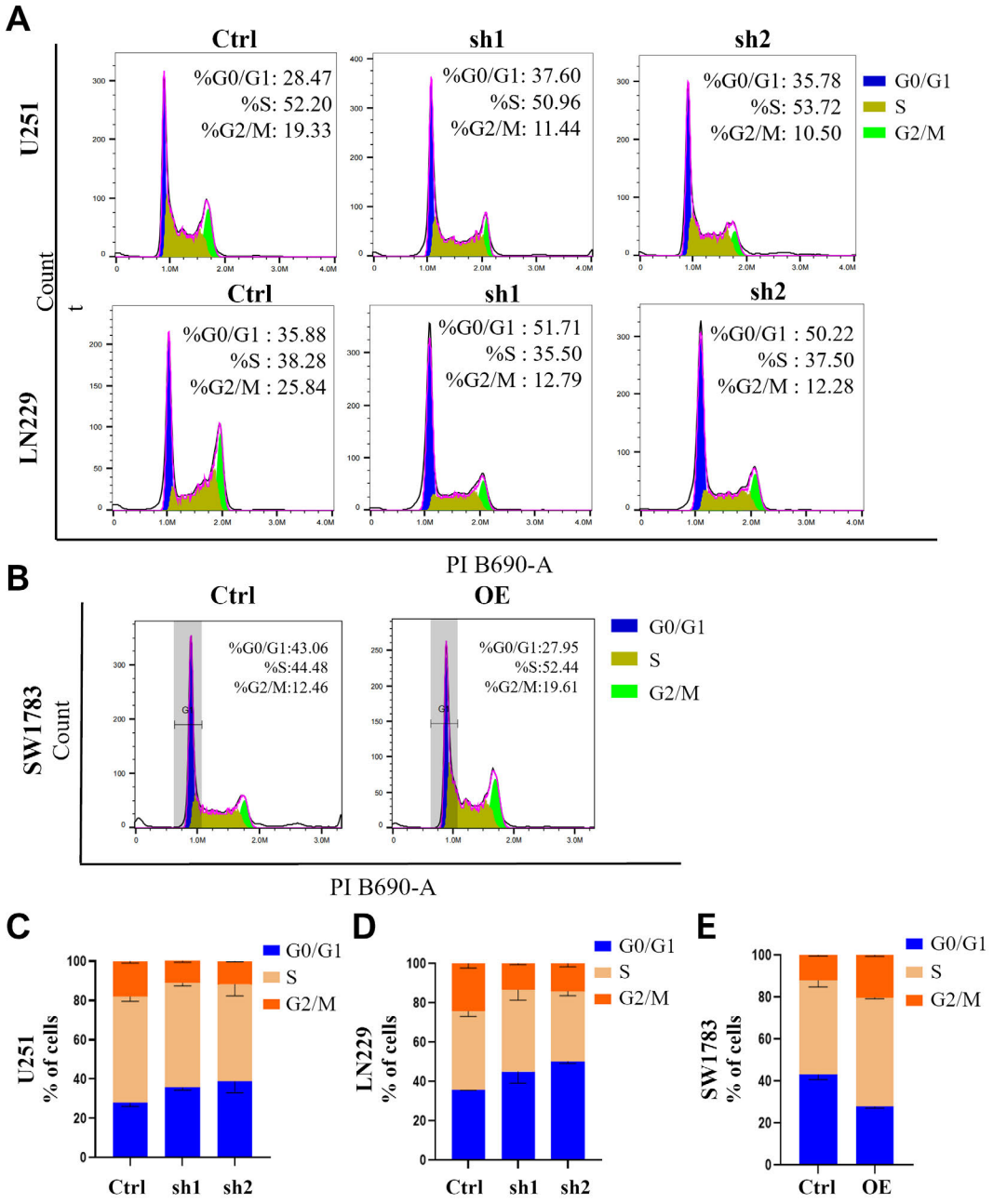

Figure 7. WDR4 knockdown induces cell-cycle arrest in G1/S phase. Knockdown of WDR4 in U251 and LN229 cells (A and C) induced G1/S arrest, and WDR4 overexpression in SW1783 cells (B and E) induced the G2/M phase transition of the cell cycle.

Oncogenes typically exert their effects by modulating key cellular signaling pathways. To investigate the potential molecular functions of WDR4 in glioma, we employed GSEA, KEGG, and GO enrichment analyses. These bioinformatic tools consistently indicated that WDR4 is closely involved in the regulation of the cell cycle. Specifically, WDR4 was enriched in pathways related to nuclear division, spindle formation, DNA-binding transcription activation, RNA polymerase II-specific activity, and other processes associated with the cell cycle of tumors. To elucidate the precise role of WDR4 in glioma, we manipulated its expression levels in glioma cell lines using knockdown and overexpression approaches. The experimental findings confirmed that upregulation of WDR4 markedly enhanced cell viability and proliferation. Conversely, WDR4 knockdown significantly suppressed glioma cell viability, proliferation, and tumori-

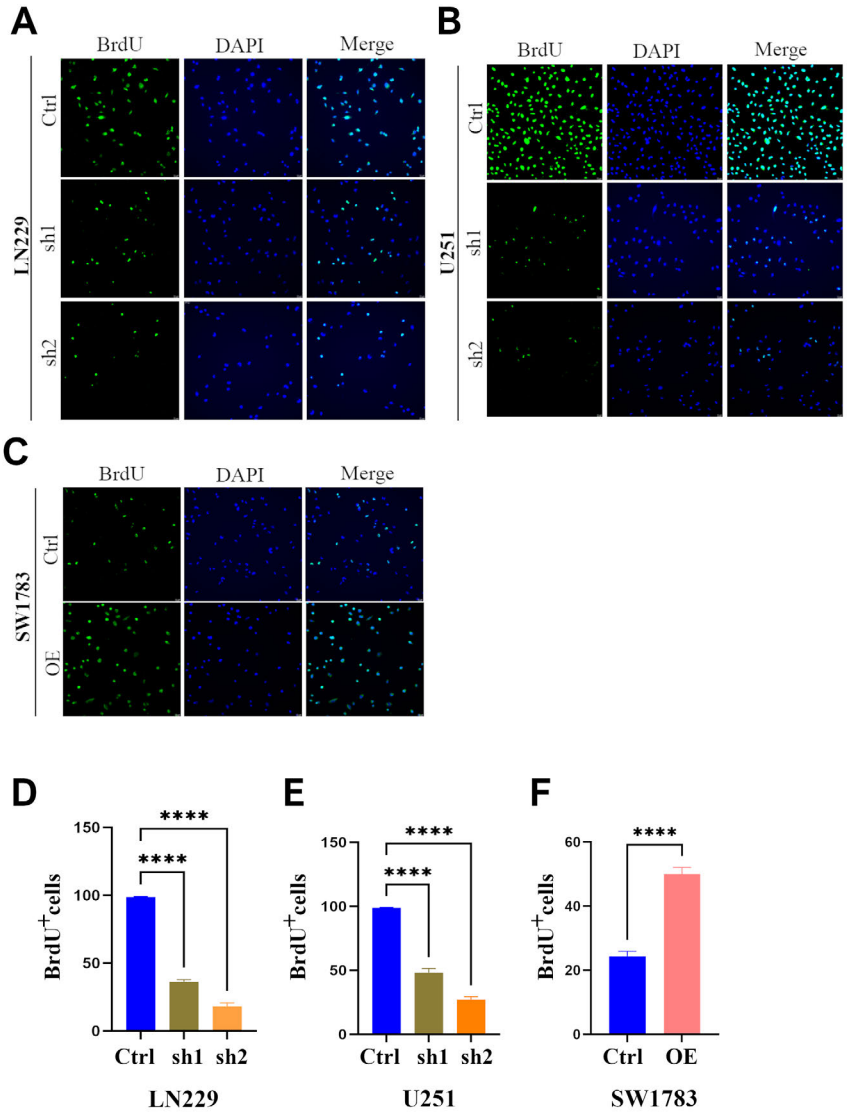

Figure 8. WDR4 knockdown inhibits BrdU incorporation. WDR4 knockdown in U251 (A and D), LN229 cells (B and E), and overexpression in SW1783 cells (C and F) were evaluated by BrdU assays.

genic potential. These results further underscore the critical role of WDR4 in regulating tumor progression in glioma. To further evaluate the tumorigenic potential of WDR4 *in vivo*, we established an intracranial xenograft glioma model using nude mice. Glioma cells with stable WDR4 knockdown or control vector were stereotactically implanted into the brains of nude mice. Bioluminescence imaging and histological analysis revealed that WDR4-silenced tumors exhibited significantly reduced growth, smaller tumor volume, and prolonged survival compared to the control group. These *in vivo* results complement our *in vitro* findings and confirm that WDR4 is a critical driver of glioma growth and malignancy under physiologically relevant conditions.

The PI3K/Akt signaling pathway is established for its critical role in regulating the survival, growth, and metabolism of tumor cells across various cancer types [25–30]. Our findings align with this model. Pearson correlation analysis revealed a positive association between WDR4 expression and the key signaling molecules CDK1, CDK2, Akt1, and Akt2. CDK1 and CDK2 are pivotal members of the cyclin-dependent kinase family, and their overexpression has been consistently linked with aggressive tumor phenotypes and poor clinical prognosis [31–34]. To further elucidate whether WDR4 influences the cell cycle and the PI3K/Akt signaling pathway in glioma cells, we conducted *in vitro* experiments. Flow cytometry and BrdU incorporation analyses demonstrated that WDR4 knockdown induced G2/M cell cycle arrest and reduced DNA synthesis, whereas WDR4 overexpression accelerated cell cycle progression. Western blot analysis further demonstrated that the knock-

down of WDR4 resulted in a reduction of CDK1 and CDK2 expression levels, as well as a decrease in Akt phosphorylation. Conversely, overexpression of WDR4 led to an increase in the expression levels of CDK1, CDK2, and phosphorylated Akt in LGG cell lines.

These findings indicate that WDR4 facilitates glioma cell proliferation by activating the PI3K/Akt signaling pathway, which in turn upregulates CDK1 and CDK2, thereby promoting cell cycle progression. This mechanistic insight highlights the critical role of the WDR4–PI3K/Akt–CDK1/2 axis in gliomagenesis and provides a potential molecular basis for therapeutic intervention.

In conclusion, this study elucidates that the elevated expression of WDR4 in glioma is significantly correlated with poor patient prognosis, indicating that WDR4 may function as an independent prognostic biomarker. Mechanistically, WDR4 modulates glioma cell cycle progression via the PI3K-Akt/CDK1/2 signaling pathway, thereby facilitating tumor cell proliferation and progression. Importantly, this research provides the first comprehensive insight into the functional role of WDR4 and its associated signaling mechanisms in glioma, offering novel theoretical foundations and potential therapeutic targets for molecularly targeted treatment of glioma. Further in-depth investigation into the precise molecular mechanisms and clinical applicability of WDR4 may advance the development of innovative and optimized therapeutic strategies for glioma management.

Acknowledgments: This work was funded by the National Natural Science Foundation (82272703, 82204456), the Training Program for Key Academic and Technical Leaders in Major Disciplines in Jiangxi Province (Young Talent Project) (20225BCJ23001), the Jiangxi Provincial Natural Science Foundation (No.20224BAB206069), the Jiangxi Province High-level and High-skilled Leading Talents Training Project (2021), the President Foundation of Nanfang Hospital, Southern Medical University (2022A003) and the Natural Science Foundation of Guangdong Province (2024A1515012949).

References

[1] LOUIS DN, ARIE PERRY A, REIFENBERGER G, VON DEIMLING A, FIGARELLA-BRANGER D et al. The 2016 World Health Organization Classification of Tumors of the Central Nervous System: a summary. Acta Neuropathol 2016; 131: 803–820. https://doi.org/10.1007/s00401-016-1545-1

[2] HORBINSKI C, BERGER T, PACKER RJ, WEN PY. Clinical implications of the 2021 edition of the WHO classification of central nervous system tumours. Nat Rev Neurol 2022; 18: 515–529. https://doi.org/10.1038/s41582-022-00679-w

[3] ŚLEDZIŃSKA P, BEBYN M, FURTAK J, KOPER A, KOPER K. Current and promising treatment strategies in glioma. Rev Neurosci 2022; 34: 483–516. https://doi.org/10.1515/revneuro-2022-0060

[4] POUYAN A, GHORBANLO M, ESLAMI M, JAHANSHAHI M, ZIAEI E et al. Glioblastoma multiforme: insights into pathogenesis, key signaling pathways, and therapeutic strategies. Mol Cancer 2025; 24: 58. https://doi.org/10.1186/s12943-025-02267-0

[5] JAIN BP, PANDEY S. WD40 Repeat Proteins: Signalling Scaffold with Diverse Functions. Protein J 2018; 37: 391–406. https://doi.org/10.1007/s10930-018-9785-7

[6] SMITH TF, GAITATZES C, SAXENA K, NEER EJ. The WD repeat: a common architecture for diverse functions. Trends Biochem Sci 1999; 24: 181–185. https://doi.org/10.1016/s0968-0004(99)01384-5

[7] LI D, ROBERTS R. WD-repeat proteins: structure characteristics, biological function, and their involvement in human diseases. Cell Mol Life Sci 2001; 58: 2085–2097. https://doi.org/10.1007/pl00000838

[8] SCHAPIRA M, TYERS M, TORRENT M, ARROWSMITH CH. WD40 repeat domain proteins: a novel target class? Nat Rev Drug Discov 2017; 16: 773–786. https://doi.org/10.1038/nrd.2017.179

[9] LUO Y, TIAN W, KANG D, WU L, TANG H et al. RNA modification gene WDR4 facilitates tumor progression and immunotherapy resistance in breast cancer. J Adv Res 2025; 72: 333–351. https://doi.org/10.1016/j.jare.2024.06.029

[10] DONG R, WANG C, TANG B, CHENG Y, PENG X et al. WDR4 promotes HCC pathogenesis through N(7)-methylguanosine by regulating and interacting with METTL1. Cell Signal 2024; 118: 111145. https://doi.org/10.1016/j.cellsig.2024.111145

[11] WANG H, LIANG L, WANG Y, ZHONG X, ZHANG C et al. WDR4 promotes colorectal cancer progression by activating the GSK3β/β-catenin pathway. Biochem Cell Biol 2025; 103: 1–12. https://doi.org/10.1139/bcb-2024-0168

[12] ZHAO P, XIA L, CHEN D, XU W, GUO H et al. METTL1 mediated tRNA m(7)G modification promotes leukaemogenesis of AML via tRNA regulated translational control. Exp Hematol Oncol 2024; 13: 8. https://doi.org/10.1186/s40164-024-00477-8

[13] XIA P, ZHANG H, XU K, JIANG X, GAO M et al. MYC-targeted WDR4 promotes proliferation, metastasis, and sorafenib resistance by inducing CCNB1 translation in hepatocellular carcinoma. Cell Death Dis 2021; 12: 691. https://doi.org/10.1038/s41419-021-03973-5

[14] WANG YT, CHEN J, CHANG CW, JEN J, HUANG TY et al. Ubiquitination of tumor suppressor PML regulates prometastatic and immunosuppressive tumor microenvironment. J Clin Invest 2017; 127: 2982–2997. https://doi.org/10.1172/JCI89957

[15] WANG G, HE X, DAI H, LIN L, CAO W et al. WDR4 promotes the progression and lymphatic metastasis of bladder cancer via transcriptional down-regulation of ARRB2. Oncogenesis 2023; 12: 47. https://doi.org/10.1038/s41389-023-00493-z

[16] ZHU J, LIU X, CHEN W, LIAO Y, LIU J et al. Association of RNA m(7)G Modification Gene Polymorphisms with Pediatric Glioma Risk. Biomed Res Int 2023; 2023: 3678327. https://doi.org/10.1155/2023/3678327

[17] CHEN Y, LIN H, MIAO L, HE J. Role of N7-methylguanosine (m(7)G) in cancer. Trends Cell Biol 2022; 32: 819–824. https://doi.org/10.1016/j.tcb.2022.07.001

[18] MA J, HAN H, HUANG Y, YANG C, ZHENG S et al. METTL1/WDR4-mediated m(7)G tRNA modifications and m(7)G codon usage promote mRNA translation and lung cancer progression. Mol Ther 2021; 29: 3422–3435. https://doi.org/10.1016/j.ymthe.2021.08.005

[19] DAI Z, LIU H, LIAO J, HUANG C, REN X et al. N(7)-Methylguanosine tRNA modification enhances oncogenic mRNA translation and promotes intrahepatic cholangiocarcinoma progression. Mol Cell 2021; 81: 3339–3355.e8. https://doi.org/10.1016/j.molcel.2021.07.003

[20] CHEN Z, ZHU W, ZHU S, SUN K, LIAO J et al. METTL1 promotes hepatocarcinogenesis via m(7) G tRNA modification-dependent translation control. Clin Transl Med 2021; 11: e661. https://doi.org/10.1002/ctm2.661

[21] CHEN B, JIANG W, HUANG Y, ZHANG J, YU P et al. N(7)-methylguanosine tRNA modification promotes tumorigenesis and chemoresistance through WNT/β-catenin pathway in nasopharyngeal carcinoma. Oncogene 2022; 41: 2239–2253. https://doi.org/10.1038/s41388-022-02250-9

[22] KONG D, SHI J, LAI C, HU J, MULATI Y et al. Comprehensive analysis of m7G-related genes METTL1 and WDR4 for predicting prognosis and oncogenic functions in prostate cancer. Discov Oncol 2025; 16: 1017. https://doi.org/10.1007/s12672-025-02847-y

[23] LIU Z, WANG X, HU B, ZHANG S, LANG Y et al. [Preliminary analysis of mRNA m7G modifications in human Adenocarcinoma of esophagogastric junction]. Zhonghua Yi Xue Yi Chuan Xue Za Zhi 2025; 42: 187–197. https://doi.org/10.3760/cma.j.cn511374-20240724-00408

[24] ZENG H, XU S, XIA E, HIRACHAN S, BHANDARI A et al. Aberrant expression of WDR4 affects the clinical significance of cancer immunity in pan-cancer. Aging (Albany NY) 2021; 13: 18360–18375. https://doi.org/10.18632/aging.203284

[25] ZHAO HF, WANG J, SHAO W, WU CP, CHEN ZP et al. Recent advances in the use of PI3K inhibitors for glioblastoma multiforme: current preclinical and clinical development. Mol Cancer 2017; 16: 100. https://doi.org/10.1186/s12943-017-0670-3

[26] COURTNEY KD, CORCORAN RB, ENGELMAN JA. The PI3K pathway as drug target in human cancer. J Clin Oncol 2010; 28: 1075–1083. https://doi.org/10.1200/JCO.2009.25.3641

[27] HE Y, SUN MM, ZHANG GG, YANG J, CHEN KS et al. Targeting PI3K/Akt signal transduction for cancer therapy. Signal Transduct Target Ther 2021; 6: 425. https://doi.org/10.1038/s41392-021-00828-5

[28] FRESNO VARA JA, CASADO E, DE CASTRO J, CEJAS P, BELDA-INIESTA C et al. PI3K/Akt signalling pathway and cancer. Cancer Treat Rev 2004; 30: 193–204. https://doi.org/10.1016/j.ctrv.2003.07.007

[29] KHEZRI MR, HSUEH HY, MOHAMMADIPANAH S, KHALILI FARD J, GHASEMNEJAD-BERENJI M. The interplay between the PI3K/AKT pathway and circadian clock in physiologic and cancer-related pathologic conditions. Cell Prolif 2024; 57: e13608. https://doi.org/10.1111/cpr.13608

[30] HUANG L, SUN J, MA Y, CHEN H, TIAN C et al. MSI2 regulates NLK-mediated EMT and PI3K/AKT/mTOR pathway to promote pancreatic cancer progression. Cancer Cell Int 2024; 24: 273. https://doi.org/10.1186/s12935-024-03444-9

[31] ZENG K, LI W, WANG Y, ZHANG Z, ZHANG L et al. Inhibition of CDK1 Overcomes Oxaliplatin Resistance by Regulating ACSL4-mediated Ferroptosis in Colorectal Cancer. Adv Sci (Weinh) 2023; 10: e2301088. https://doi.org/10.1002/advs.202301088

[32] ZHANG J, GAN Y, LI H, YIN J, HE X et al. Inhibition of the CDK2 and Cyclin A complex leads to autophagic degradation of CDK2 in cancer cells. Nat Commun 2022; 13: 2835. https://doi.org/10.1038/s41467-022-30264-0

[33] ZOU Y , XU L, WANG W, ZHU X, LIN J et al. Muscone restores anoikis sensitivity in TMZ-resistant glioblastoma cells by suppressing TOP2A via the EGFR/Integrin β1/FAK signaling pathway. Phytomedicine 2024; 129: 155714. https://doi.org/10.1016/j.phymed.2024.155714

[34] HUANG Y, SUN W, ZHU D, LIU L, FENG J et al. RBM3 Inhibits the Cell Cycle of Cutaneous Squamous Cell Carcinoma through the PI3K/AKT Signaling Pathway. Curr Mol Pharmacol 2024; 17: e18761429323760. https://doi.org/10.2174/0118761429323760240712050006